HHS Public Access

Author manuscript

J Magn Reson Imaging. Author manuscript; available in PMC 2016 March 22.

Published in final edited form as:

J Magn Reson Imaging. 2015 September ; 42(3): 811–817. doi:10.1002/jmri.24842.

Reproducibility of MR-Based Liver Fat Quantification Across Field Strength: Same-Day Comparison Between 1.5T and 3T in Obese Subjects

Nathan S. Artz, PhD[1,*], **William M. Haufe, BS**[2], **Catherine A. Hooker, BS**[2], **Gavin Hamilton, PhD**[2], **Tanya Wolfson, MA**[3], **Guilherme M. Campos, MD, PhD**[4], **Anthony C. Gamst, PhD**[3], **Jeffrey B. Schwimmer, MD**[2,5,6], **Claude B. Sirlin, MD**[2], and **Scott B. Reeder, MD, PhD**[1,7,8,9,10]

[1]Department of Radiology, University of Wisconsin, Madison, Wisconsin, USA

[2]Department of Radiology, University of California, San Diego, California, USA

[3]Department of Computational and Applied Statistics Laboratory, University of California, San Diego, California, USA

[4]Department of Surgery, University of Wisconsin, Madison, Wisconsin, USA

[5]Department of Pediatrics, University of California, San Diego, California, USA

[6]Department of Gastroenterology, Rady Children's Hospital, San Diego, California, USA

[7]Department of Medical Physics, University of Wisconsin, Madison, Wisconsin, USA

[8]Department of Biomedical Engineering, University of Wisconsin, Madison, Wisconsin, USA

[9]Department of Medicine, University of Wisconsin, Madison, Wisconsin, USA

[10]Department of Emergency Medicine, University of Wisconsin, Madison, Wisconsin, USA

Abstract

Purpose—To examine the reproducibility of quantitative magnetic resonance (MR) methods to estimate hepatic proton density fat-fraction (PDFF) at different magnetic field strengths.

Materials and Methods—This Health Insurance Portability and Accountability Act (HIPAA)-compliant study was approved by the Institutional Review Board. Following informed consent, 25 severely obese subjects (mean body mass index [BMI]: 45 ± 4, range: 38–53 kg/m^2) were scanned at 1.5T and 3T on the same day. Two confounder-corrected multiecho chemical shift-encoded gradient-echo-based imaging methods were acquired to estimate PDFF over the entire liver: 3D complex-based (MRI-C) and 2D magnitude-based (MRI-M) MRI. Single-voxel MR spectroscopy (MRS) was performed in the right liver lobe. Using linear regression, pairwise comparisons of estimated PDFF were made between methods (MRI-C, MRI-M, MRS) at each field strength and for each method across field strengths.

Results—1.5T vs. 3T regression analyses for MRI-C, MRI-M, and MRS PDFF measurements yielded R^2 values of 0.99, 0.97, and 0.90, respectively. The best-fit line was near unity (slope(m) =

[*]Address reprint requests to: N.S.A., Wisconsin Institutes for Medical Research, 1111 Highland Ave., Rm. 1005, Madison, WI 53705-2275. nartz@wisc.edu, nathanartz@gmail.com.

1, intercept(b) = 0), indicating excellent agreement for each case: MRI-C (m = 0.92 [0.87, 0.99], b = 1.4 [0.7, 1.8]); MRI-M (m = 1.0 [0.90, 1.08], b = −1.4 [−2.4, −0.5]); MRS (m = 0.98 [0.82, 1.15], b = 1.2 [−0.2, 3.0]). Comparing MRI-C and MRI-M yielded an R^2 = 0.98 (m = 1.1 [1.02, 1.16], b = −1.8 [−2.8, −1.1]) at 1.5T, and R^2 = 0.99 (m = 0.98 [0.93, 1.03], b = 1.2 [0.7, 1.7]) at 3T.

Conclusion—This study demonstrates that PDFF estimation is reproducible across field strengths and across two confounder-corrected MR-based methods.

Nonalcoholic fatty liver disease (NAFLD) is the most common cause of chronic liver disease, affecting between 20% to 30% of the U.S. population[1,2] and an even greater percentage of the obese population.[3] NAFLD can progress to liver inflammation, fibrosis, and eventually cirrhosis with complications including liver failure, portal hypertension, and hepatocellular carcinoma.[4] Recent studies have shown that hepatic fat content demonstrates a strong link to metabolic complications in the obese population,[5,6] and individuals with elevated liver fat are at higher risk of heart disease and diabetes.[7] Unfortunately, definitive diagnosis of NAFLD currently requires biopsy, which is expensive, carries some risk, and most important suffers from sampling variability.[8,9] Noninvasive, whole-liver fat quantification is critical for early detection and grading of NAFLD, and holds considerable potential to facilitate early intervention to prevent or reverse progression, as well as monitor treatment.

In recent years, confounder-corrected chemical-shift-encoded quantitative magnetic resonance imaging (MRI) methods have shown promise as a noninvasive biomarker of hepatic steatosis.[10–14] These methods exploit the fact that hydrogen protons in water precess at a different resonance frequency than hydrogen protons in triglycerides. When all confounding factors are addressed (vide infra), the proton density fat-fraction (PDFF), an inherent property of tissue, can be quantified.[15]

The first MR technique to demonstrate good correlation of hepatic fat content with tissue reference standards was MR spectroscopy (MRS),[16–18] and it is widely accepted as the noninvasive reference standard for fat-quantification in tissue. In recent years, the most common approach has combined a stimulated echo acquisition mode (STEAM) acquisition scheme with T_2 correction and spectral modeling that accounts for the multipeak spectral structure of hepatic triglycerides.[10] MRS has several inherent drawbacks, however, that limit its clinical utility. Spatial coverage is limited to a single voxel, leading to sampling variability, which may be problematic for longitudinal follow-up and treatment monitoring. Further, most MRS methods require advanced postprocessing by individuals with experience in MRS.

Three-dimensional imaging methods are necessary to assess fat content across the entire liver. Two independently developed confounder-corrected multiecho chemical-shift-based MRI techniques have shown promise for whole-liver PDFF quantification. One is a multislice 2D magnitude-based gradient echo method,[13,14] referred to as MRI-M for brevity, while the other is a 3D complex-based gradient echo method, referred to as MRI-C.[19] To quantify PDFF from multiple images acquired at increasing echo times, both techniques incorporate a multipeak spectral model of liver fat[10,20] and T_2* correction,[21] and both use

low flip angles to mitigate T_1 bias.[22,23] Because MRI-C uses complex data, it also corrects for eddy currents[24] and noise-related bias.[23] Numerous validation studies have been performed assessing accuracy and repeatability in phantoms, animal models, and patients for MRI-M and MRI-C.[11–14,25–29] Two MRI vendors (GE Healthcare, Waukesha, WI, Philips, Best, Netherlands) now offer MRI-C as a commercial product for quantifying hepatic fat-fraction.

Most commercially available clinical MRI scanners have 1.5T or 3T field strength. Since 1.5T and 3T field strengths are associated with different resonant frequencies, relaxation parameters, and B_0 and B_1 inhomogeneities, it is important to verify that PDFF measurements are reproducible across field strength. Because known confounders of PDFF have been addressed using MRI-M, MRI-C, and MRS, these methods should provide consistent estimates of hepatic PDFF. Some investigations have shown encouraging preliminary 1.5T vs. 3T results for one or more methods similar to those described above.[30,31] The purpose of this work was to compare MRI-C, MRI-M, and MRS hepatic PDFF measurements in obese patients at high risk for NAFLD and examine each technique's reproducibility across field strengths, specifically 1.5T and 3T.

Materials and Methods

This Health Insurance Portability and Accountability Act (HIPPA)-compliant study was approved by our institutional Human Subjects Review Committee and written informed consent was obtained from all subjects. Obese patients that were selected for weight-loss surgery were informed of the study in consecutive order during routine clinic appointments. When a patient indicated interest in further information and he/she met the inclusion criteria, recruitment commenced by telephone. We included adults (>18 years of age) who were severely obese (body mass index [BMI] >35 kg/m^2) and being evaluated for weight loss surgery. Exclusion criteria were contraindications to MRI or history of known liver disease besides potential NAFLD.

Between March 2012 and December 2013, a total of 25 subjects (21 Caucasian females; three Caucasian males; one African-American male) participated in this study (age: 48 ± 13 years; weight: 116 ± 14 kg; BMI: 45 ± 4 kg/m^2 with range 38–53 kg/m^2 and median 44 kg/m^2). Each subject was scanned at both 1.5T and 3T (Signa HDx and Discovery MR750, respectively, GE Healthcare) on the same day within a 1-hour period. The diameter of the bore was 60 cm for each scanner. An eight-channel phased array cardiac coil and a 32-channel phased array abdominal coil were used at 1.5T and 3T, respectively. At each field strength, three separate liver fat quantification methods were performed within a scanning session that was 15 minutes or less (including patient setup, localization, and calibration).

3D Complex-Based Gradient Echo Imaging (MRI-C)

A 3D complex-based multiecho chemical shift-encoded method was performed.[19] Acquisition parameters at 3T included: 6 total echoes acquired in two interleaved shots, TR = 8.6 msec, TE_1 = 1.2 msec, ΔTE = 1.0 msec, flip = 3°, BW = ±125 kHz, FOV = 44 cm, slice = 8 mm, 256 × 128 matrix, 32 slices, ARC parallel imaging acceleration = 2 × 2, and a total scan time of 20 seconds (single breath-hold). The true spatial resolution at 3T was 1.7 ×

3.4 × 8.0 mm^3, interpolated to 1.7 × 1.7 × 8 mm^3 through zero-filling. Parameters at 1.5T were similar except for the following: TR = 13.4 msec, 6 echoes all in one shot, 256 × 160 matrix, flip = 5°, TE_1 = 1.2 msec, ΔTE = 2.0 msec. The true spatial resolution at 1.5T was 1.7 × 2.8 × 8 mm^3, interpolated to 1.7 × 1.7 × 8 mm^3 through zero-filling. At both 1.5T and 3T, the choice of flip angle was based on the TR of each acquisition to minimize T_1 related bias.[26,32]

2D Magnitude-Based Gradient Echo Imaging (MRI-M)

A 2D magnitude-based gradient echo method[13,14] was also performed at both field strengths: acquisition parameters at 3T included the following: 6 echoes/TR in one shot, TR = 150 msec, TE_1 = 1.15 msec, ΔTE = 1.15 msec, flip = 10°, BW = ±125 kHz, FOV = 44 cm, slice = 8 mm, 224 × 160 matrix, 28 slices, ASSET factor = 2, for a total scan time of 26 seconds (split into two breath-holds). The true spatial resolution at 3T was 2.0 × 2.8 × 8.0 mm^3, interpolated to 1.7 × 1.7 × 8 mm^3 through zero-filling. Parameters were adjusted at 1.5T as follows: TR = 170 msec, TE_1 = 2.3 msec, ΔTE = 2.3 msec, BW = ±83 kHz, matrix = 256 × 160, ASSET factor = 1.5, total scan of 42 seconds (split into three breath-holds).

Single Voxel MRS

Single breath-hold STEAM MRS was performed in a single voxel (without spatial or water suppression) as previously described[10] at both 1.5T and 3T. A 20 × 20 × 20 mm^3 voxel was placed in the posterior segment of the right hepatic lobe (Couinaud segment 6 or 7) avoiding large biliary and vascular structures. 3T acquisition parameters included: TR = 3500 msec, five echoes with TEs (10, 15, 20, 25, 30 msec), spectral width ±2.5 kHz, 2048 points, 1 signal average, 21 seconds breath-hold. 1.5T parameters were the same except for the echo times: 10, 20, 30, 40, 50 msec.

PDFF Determination and Image Analysis

MRS—T_2-corrected MRS spectra were analyzed to estimate PDFF by a single observer with 14 years of experience (G.H.) using the AMARES algorithm, also as previously described.[10]

MRI—Reconstruction of PDFF maps from source echo images were performed online using investigational versions of the algorithms previously described for MRI-M[33] and for MRI-C.[12,29] Both algorithms use spectral modeling of fat[10,11] and T_2* correction.[12] MRI-C also corrected for eddy currents and noise-related bias.[13,14] A 3.14 cm^2 region-of-interest (ROI) was placed on the PDFF map in each of the nine Couinaud liver segments (1, 2, 3, 4a, 4b, 5, 6, 7, 8) while colocalizing the placement between 1.5T and 3T images.

The average of these nine ROI measurements was used to compare MRI-M and MRI-C at each of the field strengths and to compare each method across field strengths.

To compare MRI-M and MRI-C with MRS, additional ROIs were colocalized with the MRS voxel coordinates and averaged across the three 8 mm slices centered on the 20 mm MRS voxel. A data storage failure occurred for one 1.5T MRS file in one of the 25 subjects, precluding its use in relevant analyses.

Statistical Analyses

Univariate linear regression was used to assess agreement, pairwise, between methods and between field strengths in this study. The following relationships were evaluated in separate models: MRI-C at 3T vs. MRI-C at 1.5T, MRI-M at 3T vs. MRI-M at 1.5T, MRS at 3T vs. MRS at 1.5T, MRI-C at 1.5T vs. MRI-M at 1.5T, MRI-C at 3T vs. MRI-M at 3T, MRS at 1.5T vs. MRI-C at 1.5T, MRS at 3T vs. MRI-C at 3T, MRS at 1.5T vs. MRI-M at 1.5T, MRS at 3T vs. MRI-M at 3T. For each regression model the intercept and slope of the regression line, the coefficient of determination R^2, and the average bias were computed. Average bias is defined as the square root of the average squared difference between the regression line and the Y = X line of unity. Bootstrap-based bias-corrected accelerated 95% confidence intervals (CI) were computed for each parameter.

Results

Representative PDFF maps are displayed in Fig. 1 for MRI-M and MRI-C at 1.5T and 3T for a subject with low hepatic fat content and in a subject with high hepatic fat content. Excellent agreement was observed both qualitatively and quantitatively, with minimal variation between colocalized liver PDFF measurements. Note that MRI-M is capable of measuring PDFF from 0 to 50%, while MRI-C can measure PDFF from 0–100%. This difference in dynamic range between MRI-C and MRI-M explains the difference in appearance of adipose tissue outside the liver, which typically has PDFF exceeding 90%.

Excellent correlation and agreement was observed between 3T and 1.5T for all three MR-based PDFF techniques (Fig. 2). The R^2 values for MRI-C, MRI-M, and MRS were 0.99, 0.97, and 0.90, respectively, suggesting that MRS may demonstrate the most variability between the two field strengths. The slope and intercept (m = slope [95% CI], b = intercept [95% CI]) were also near one and zero for MRI-C (m = 0.92 [0.87, 0.99], b = 1.4 [0.7, 1.8]) and MRI-M (m = 1.0 [0.90, 1.08], b = −1.4 [−2.4, −0.5]), although perfect agreement (m = 1 and b = 0) was not achieved in either case. At low fat-fractions, 3T MRI-C measurements were slightly larger than those at 1.5T, leading to a positive intercept and slope less than one. MRI-M measurements exhibited an average bias of 1.4% between field strengths. Despite more variability and lower correlation, confidence intervals for 3T MRS vs. 1.5T MRS included a slope of one and intercept of zero (m = 0.98 [0.82, 1.15], b = 1.2 [−0.2, 3.0]).

Comparison of complex-based and magnitude-based PDFF measurements (Fig. 3) yielded excellent correlation at 1.5T (R^2 = 0.98) and 3T (R^2 = 0.99). Agreement was very good at 1.5T (m = 1.1 [1.02, 1.16], b = −1.8 [−2.8, −1.1]), but not perfect, as MRI-C measured lower values compared to MRI-M in the region of low PDFF. 3T MRI-C vs. 3T MRI-M also agreed very well (m = 0.98 [0.93, 1.03], b = 1.2 [0.7, 1.7]), although an average bias of ~1% existed across all measured fat-fractions.

MRS-based PDFF measurements were also compared to those made by MRI-C at 1.5T and 3T (Fig. 4) and MRI-M at 1.5T and 3T (Fig. 5). The goodness of fit was excellent ($R^2 \geq$ 0.94) in all cases. MRS and MRI-C PDFF measurements at 1.5T deviated with larger fat-fractions, causing the slope to differ marginally from unity (m = 0.86 [0.78, 0.96], b = −0.03

[−0.9, 1.3]). Regression for MRS vs. MRI-C at 3T (m = 0.98 [0.90, 1.06], b = −1.1 [−2.0, −0.05]) fell only slightly below unity with an average bias of ~1.4% for all fat-fractions. Comparing MRS to MRI-M at 1.5T (m = 0.95 [0.83, 1.10], b = −2.3 [−3.8, −0.5]) yielded a consistent bias averaging ~2.9% for all fat-fractions. Near-perfect agreement was observed between MRS and MRI-M at 3T (m = 1.00 [0.91, 1.08], b = 0.2 [−0.6, 1.3]) where the best-fit line was not statistically different from the line of unity.

Discussion

This work demonstrates that MR-based estimation of hepatic PDFF is reproducible across the two most common clinically available field strengths (1.5T and 3T) in obese subjects. Although agreement was not perfect in all cases, only small biases led to deviation from unity. Further, excellent reproducibility between two different MRI methods, a 2D magnitude-based method (MRI-M) and a 3D complex-based method (MRI-C), was shown. This demonstrates through a direct comparison that when confounders are addressed, estimation of PDFF is reproducible across imaging method. Excellent agreement across field strength and method allows great flexibility for noninvasive detection, grading, and longitudinal evaluation of fatty liver disease.

The demonstration of reproducibility of PDFF quantification in obese subjects is clinically relevant. This population is at an elevated risk of NAFLD and is a patient group that may benefit from noninvasive detection and grading of liver fat. Further, with the increasing recognition of bariatric weight loss surgery as an effective means to treat the metabolic syndrome[34,35] noninvasive methods for longitudinal evaluation of liver fat are increasingly relevant.

Scanning obese subjects can be challenging, particularly in smaller bore (eg, 60 cm) magnets with table weight limits (eg, 136 kg). In addition, the increased distance from the liver to elements of the radiofrequency coils reduces the signal-to-noise ratio (SNR) performance of MR-based methods. Further, short scanning protocols are critical, as close-fitting conditions become rapidly uncomfortable with time. The scanning session in this study was ≤15 minutes.

Whole-liver PDFF measurements demonstrated higher correlation (ie, less variation) for the 1.5T vs. 3T data compared to the single-voxel MRS technique. This is likely due to unavoidable variation in voxel placement between 1.5T and 3T scans, which is an inherent drawback of MRS when performing repeated studies. Further, numerous factors that can confound PDFF measurement (eg, T_1, T_2, T_2*, spectral complexity of fat, eddy currents, noise) were accounted for in this study, yet small differences remain between PDFF techniques and between field strengths. The largest difference was between MRS and MRI-M at 1.5T. The source of this bias is under investigation, but it is plausibly due in part to low SNR of the M-MRI method at 1.5T, as near-perfect agreement was observed at 3T between MRS and MRI-M. The small but statistically significant differences from the line of unity observed in this work indicate that some of the PDFF methods did not perfectly correct all confounding factors. It is unknown whether these small remaining discrepancies are clinically relevant in the low PDFF realm.

There were several limitations to this study, including the relatively small number of subjects. Although the statistical results of this study demonstrate strong 1.5T vs. 3T agreement, additional reproducibility studies including other patient populations are needed. Although this study was limited to one patient population, we consider the demonstration of reproducibility of MR-based PDFF measurements in obese subjects a strength, given the challenges associated with imaging such patients. Further work is also needed to validate the accuracy of PDFF measurements with tissue reference standards, such as histology and triglyceride analysis. In addition, future validation studies should be performed at multiple sites and on multiple vendor platforms.

In conclusion, this study demonstrated excellent reproducibility for MR-based PDFF measurements in the liver across field strength (1.5T and 3.0T) and between two different confounder-corrected methods. These results suggest that noninvasive, longitudinal evaluation of whole-liver fat content can be performed interchangeably between 1.5 and 3T and between magnitude- or complex-based methods.

Acknowledgments

The authors thank Chris Roginski for patient recruitment and coordination, our MR research technologists, Sara Pladziewicz and Jenelle Fuller, for performing the volunteer scans, and GE Healthcare for research support.

Contract grant sponsor: National Institutes of Health; Contract grant number: R01 DK088925-01.

References

1. Boyce CJ, Pickhardt PJ, Kim DH, et al. Hepatic steatosis (fatty liver disease) in asymptomatic adults identified by unenhanced low-dose CT. AJR Am J Roentgenol. 2010; 194:623–628. [PubMed: 20173137]
2. Szczepaniak LS, Nurenberg P, Leonard D, et al. Magnetic resonance spectroscopy to measure hepatic triglyceride content: prevalence of hepatic steatosis in the general population. Am J Physiol Endocrinol Metab. 2005; 288:E462–468. [PubMed: 15339742]
3. Browning JD, Szczepaniak LS, Dobbins R, et al. Prevalence of hepatic steatosis in an urban population in the United States: impact of ethnicity. Hepatology. 2004; 40:1387–1395. [PubMed: 15565570]
4. Ekstedt M, Franzén LE, Mathiesen UL, et al. Long-term follow-up of patients with NAFLD and elevated liver enzymes. Hepatology. 2006; 44:865–873. [PubMed: 17006923]
5. Fabbrini E, Magkos F, Mohammed BS, et al. Intrahepatic fat, not visceral fat, is linked with metabolic complications of obesity. Proc Natl Acad Sci U S A. 2009; 106:15430–15435. [PubMed: 19706383]
6. Alderete TL, Toledo-Corral CM, Desai P, Weigensberg MJ, Goran MI. Liver fat has a stronger association with risk factors for type 2 diabetes in African-American compared with Hispanic adolescents. J Clin Endocrinol Metab. 2013; 98:3748–3754. [PubMed: 23873990]
7. Targher G, Day CP, Bonora E. Risk of cardiovascular disease in patients with nonalcoholic fatty liver disease. N Engl J Med. 2010; 363:1341–1350. [PubMed: 20879883]
8. Ratziu V, Charlotte F, Heurtier A, et al. Sampling variability of liver biopsy in nonalcoholic fatty liver disease. Gastroenterology. 2005; 128:1898–1906. [PubMed: 15940625]
9. Bedossa P, Dargere D, Paradis V. Sampling variability of liver fibrosis in chronic hepatitis C. Hepatology. 2003; 38:1449–1457. [PubMed: 14647056]
10. Hamilton G, Yokoo T, Bydder M, et al. In vivo characterization of the liver fat (1)H MR spectrum. NMR Biomed. 2011; 24:784–790. [PubMed: 21834002]
11. Hines CD, Yu H, Shimakawa A, et al. Quantification of hepatic steatosis with 3-T MR imaging: validation in ob/ob mice. Radiology. 2010; 254:119–128. [PubMed: 20032146]

12. Meisamy S, Hines CD, Hamilton G, et al. Quantification of hepatic steatosis with T1-independent, T2-corrected MR imaging with spectral modeling of fat: blinded comparison with MR spectroscopy. Radiology. 2011; 258:767–775. [PubMed: 21248233]
13. Yokoo T, Bydder M, Hamilton G, et al. Nonalcoholic fatty liver disease: diagnostic and fat-grading accuracy of low-flip-angle multiecho gradient-recalled-echo MR imaging at 1.5 T. Radiology. 2009; 251:67–76. [PubMed: 19221054]
14. Yokoo T, Shiehmorteza M, Hamilton G, et al. Estimation of hepatic proton-density fat fraction by using MR imaging at 3.0 T. Radiology. 2011; 258:749–759. [PubMed: 21212366]
15. Reeder SB, Hu HH, Sirlin CB. Proton density fat-fraction: a standardized MR-based biomarker of tissue fat concentration. J Magn Reson Imaging. 2012; 36:1011–1014. [PubMed: 22777847]
16. Longo R, Pollesello P, Ricci C, et al. Proton MR spectroscopy in quantitative in vivo determination of fat content in human liver steatosis. J Magn Reson Imaging. 1995; 5:281–285. [PubMed: 7633104]
17. Szczepaniak LS, Babcock EE, Schick F, et al. Measurement of intracellular triglyceride stores by H spectroscopy: validation in vivo. Am J Physiol. 1999; 276(5 Pt 1):E977–989. [PubMed: 10329993]
18. Thomsen C, Becker U, Winkler K, Christoffersen P, Jensen M, Henriksen O. Quantification of liver fat using magnetic resonance spectroscopy. Magn Reson Imaging. 1994; 12:487–495. [PubMed: 8007779]
19. Reeder SB, McKenzie CA, Pineda AR, et al. Water-fat separation with IDEAL gradient-echo imaging. J Magn Reson Imaging. 2007; 25:644–652. [PubMed: 17326087]
20. Yu H, Shimakawa A, McKenzie CA, Brodsky E, Brittain JH, Reeder SB. Multiecho water-fat separation and simultaneous R2* estimation with multifrequency fat spectrum modeling. Magn Reson Med. 2008; 60:1122–1134. [PubMed: 18956464]
21. Yu H, McKenzie CA, Shimakawa A, et al. Multiecho reconstruction for simultaneous water-fat decomposition and T2* estimation. J Magn Reson Imaging. 2007; 26:1153–1161. [PubMed: 17896369]
22. Hines CD, Yu H, Shimakawa A, McKenzie CA, Brittain JH, Reeder SB. T1 independent, T2* corrected MRI with accurate spectral modeling for quantification of fat: validation in a fat-water-SPIO phantom. J Magn Reson Imaging. 2009; 30:1215–1222. [PubMed: 19856457]
23. Liu CY, McKenzie CA, Yu H, Brittain JH, Reeder SB. Fat quantification with IDEAL gradient echo imaging: correction of bias from T(1) and noise. Magn Reson Med. 2007; 58:354–364. [PubMed: 17654578]
24. Yu H, Shimakawa A, Hines CD, et al. Combination of complex-based and magnitude-based multiecho water-fat separation for accurate quantification of fat-fraction. Magn Reson Med. 2011; 66:199–206. [PubMed: 21695724]
25. Kang BK, Yu ES, Lee SS, et al. Hepatic fat quantification: a prospective comparison of magnetic resonance spectroscopy and analysis methods for chemical-shift gradient echo magnetic resonance imaging with histologic assessment as the reference standard. Invest Radiol. 2012; 47:368–375. [PubMed: 22543969]
26. Johnson BL, Schroeder ME, Wolfson T, et al. Effect of flip angle on the accuracy and repeatability of hepatic proton density fat fraction estimation by complex data-based, T1-independent, T2*-corrected, spectrum-modeled MRI. J Magn Reson Imaging. 2014; 39:440–447. [PubMed: 23596052]
27. Kuhn JP, Hernando D, Munoz del Rio A, et al. Effect of multipeak spectral modeling of fat for liver iron and fat quantification: correla tion of biopsy with MR imaging results. Radiology. 2012; 265:133–142. [PubMed: 22923718]
28. Hines CD, Agni R, Roen C, et al. Validation of MRI biomarkers of hepatic steatosis in the presence of iron overload in the ob/ob mouse. J Magn Reson Imaging. 2012; 35:844–851. [PubMed: 22127834]
29. Hines CD, Frydrychowicz A, Hamilton G, et al. T(1) independent, T(2) (*) corrected chemical shift based fat-water separation with multi-peak fat spectral modeling is an accurate and precise measure of hepatic steatosis. J Magn Reson Imaging. 2011; 33:873–881. [PubMed: 21448952]

30. Hansen KH, Schroeder ME, Hamilton G, Sirlin CB, Bydder M. Robustness of fat quantification using chemical shift imaging. Magn Reson Imaging. 2012; 30:151–157. [PubMed: 22055856]
31. Kang GH, Cruite I, Shiehmorteza M, et al. Reproducibility of MRI-determined proton density fat fraction across two different MR scanner platforms. J Magn Reson Imaging. 2011; 34:928–934. [PubMed: 21769986]
32. Hines, CD.; Yokoo, T.; Bydder, M.; Sirlin, CB.; Reeder, SB. Optimization of flip angle to allow tradeoffs in T1 bias and SNR performance for fat quantification.. Proc 18th Annual Meeting ISMRM; Stockholm. 2010; p. 224
33. Bydder M, Yokoo T, Hamilton G, et al. Relaxation effects in the quantification of fat using gradient echo imaging. Magn Reson Imaging. 2008; 26:347–359. [PubMed: 18093781]
34. Buchwald H, Estok R, Fahrbach K, et al. Weight and type 2 diabetes after bariatric surgery: systematic review and meta-analysis. Am J Med. 2009; 122:248–256. e245. [PubMed: 19272486]
35. Schauer PR, Kashyap SR, Wolski K, et al. Bariatric surgery versus intensive medical therapy in obese patients with diabetes. N Engl J Med. 2012; 366:1567–1576. [PubMed: 22449319]

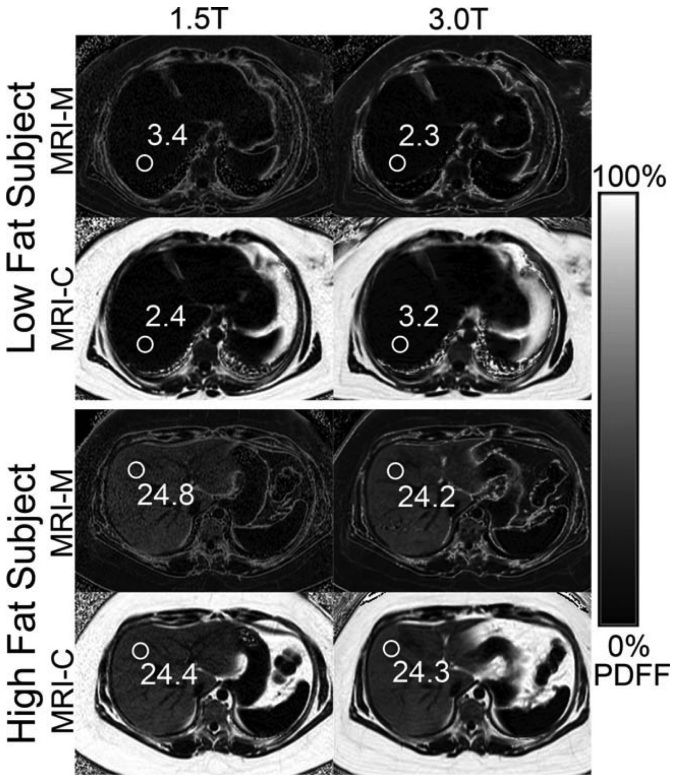

FIGURE 1.

Excellent qualitative and quantitative agreement was observed in whole-liver PDFF maps between magnetic field strengths and between MRI-M and MRI-C. Colocalized measurements are displayed for two subjects, one with low hepatic fat content (top) and one with high hepatic fat content (bottom). The differences in dynamic range for MRI-M (0–50%) and MRI-C (0–100%) explain the difference in appearance of the subcutaneous tissue which typically has PDFF >90%.

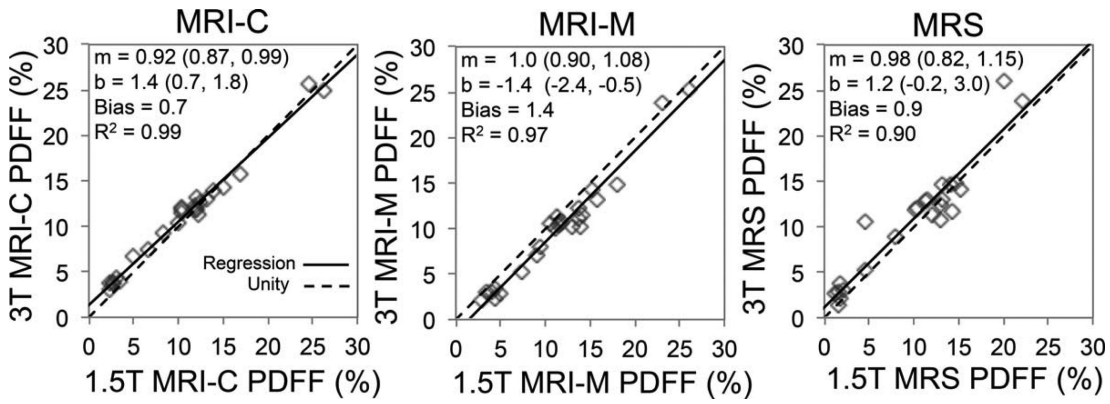

FIGURE 2.

Excellent correlation and agreement was observed between 3T and 1.5T for all three liver PDFF techniques. The imaging techniques demonstrated less variability than MRS, and the slope (m) and intercept (b) were close to one and zero. At low fat-fractions, 3T MRI-C measurements were slightly larger than those at 1.5T. A small systematic bias was observed for MRI-M between field strengths. Confidence intervals for MRS include a slope of one and intercept of zero, although with higher variability.

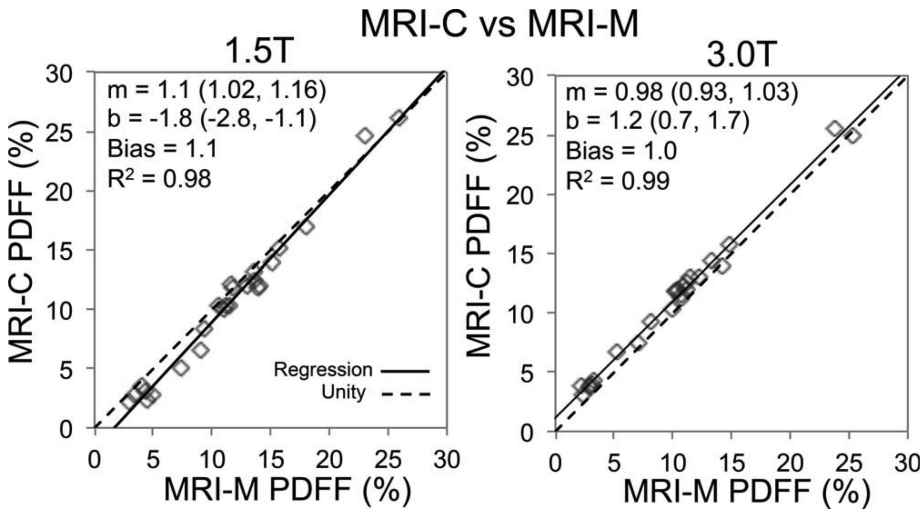

FIGURE 3.

Complex-based (MRI-C) and magnitude-based (MRI-M) PDFF measurements demonstrated excellent agreement at 1.5T and 3T. A slight deviation from unity is observed in the lower fat-fractions at 1.5T, while a small (~1%), systematic bias was observed at 3T.

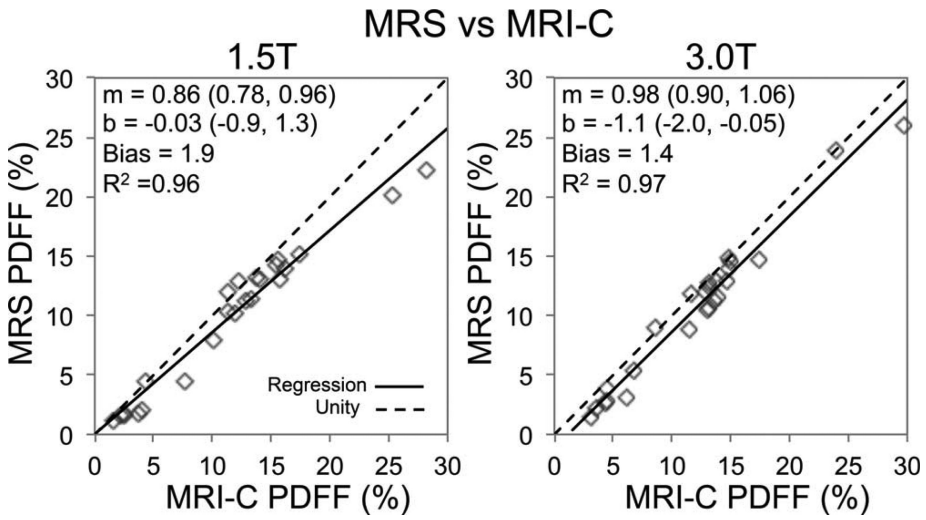

FIGURE 4.

Complex-based MRI PDFF measurements showed excellent correlation with MRS at 1.5T and 3T. At 1.5T, a deviation from unity with increasing fat-fractions was observed, leading to a slope that was statistically different than unity. The regression line for 3T was just below the line of unity, with an average bias of 1.4%.

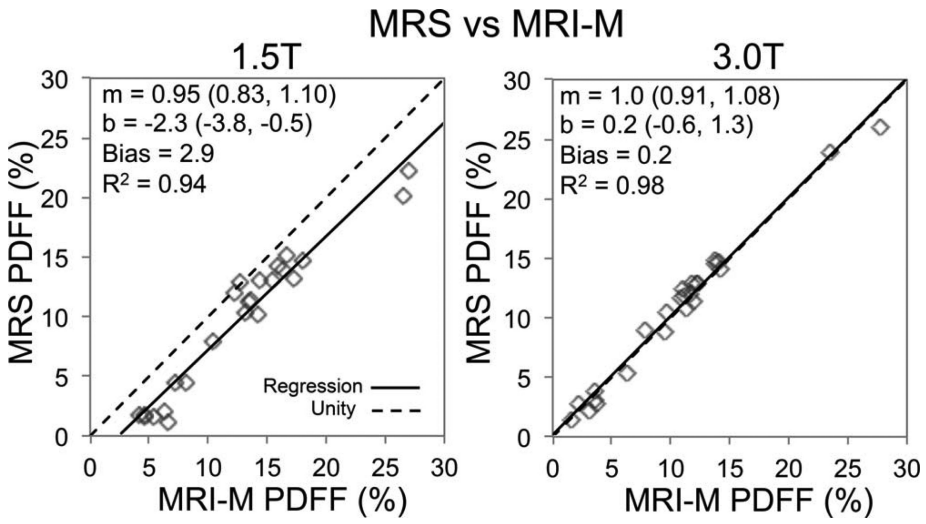

FIGURE 5.

Magnitude-based MRI PDFF measurements demonstrated perfect agreement with MRS at 3T, while 1.5T measurements demonstrated excellent correlation with a systematic bias of ~2.9%.